Journal of Scientific Computing (2023) 95:57
https://doi.org/10.1007/s10915-023-02187-5

A viscoelastic Timoshenko Beam Model: Regularity and Numerical Approximation

Yiqun Li[1] · Hong Wang[1] · Xiangcheng Zheng[2]

Received: 20 October 2022 / Revised: 3 March 2023 / Accepted: 20 March 2023 /
Published online: 7 April 2023

Abstract
We derive a fully-discrete finite element scheme to a fractional Timoshenko beam model, which characterizes the mechanical responses of viscoelastic beams, thick beams and beams subject to high-frequency excitations by properly considering the effects of both transverse shear and rotational inertia. We prove high-order regularity of the solutions to the model and then accordingly prove error estimates of the numerical scheme. Numerical experiments are performed to substantiate the numerical analysis results and to demonstrate the effectiveness of the fractional Timoshenko beam model in modeling the mechanical vibrations of different beams, in comparison with its integer-order analogue and the widely-used integer-order and fractional Euler-Bernoulli beam models.

Keywords Fractional Timoshenko beam model · Viscoelasticity · Regularity · Finite element approximation · Error estimate

Mathematics Subject Classification 35S10 · 45K05 · 65M60

1 Introduction

Viscoelastic materials such as polymeric materials and natural fibers exhibit mechanical properties intermediate between those of viscous liquid and elastic solid when undergoing deformation, and have shown widespread applications [3, 8, 24, 25]. In particular, numerous experiments indicate that viscoelastic materials demonstrate power-law behaviors [2, 5, 31, 33, 40]. For instance, classical rheological models combine elastic elements (Hooke's

✉ Xiangcheng Zheng
xzheng@sdu.edu.cn

Yiqun Li
yiqunl@email.sc.edu

Hong Wang
hwang@math.sc.edu

[1] Department of Mathematics, University of South Carolina, Columbia, SC 29208, USA

[2] School of Mathematics, Shandong University, Jinan 250100, China

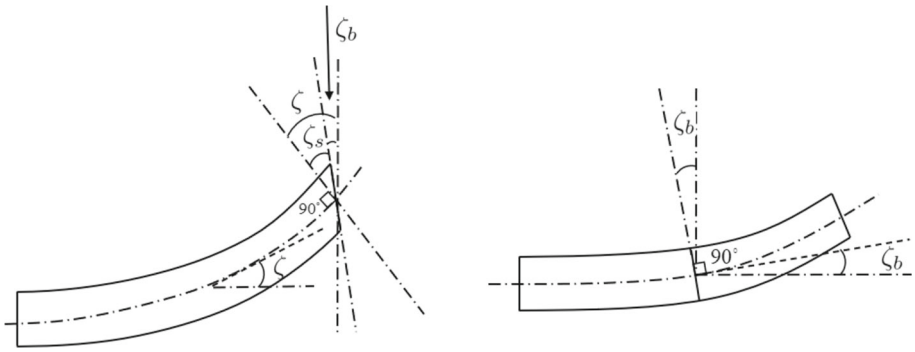

Fig. 1 Bending behavior of Timoshenko (left) and Euler-Bernoulli (right) beams

springs) with viscous components (Newtonian dashpots) to mimic the mixed properties of the viscoelastic materials, which fundamentally approximate their power-law behaviors by a combination of decaying exponentials [2, 5, 15, 24, 34]. Consequently, the fractional viscoelastic models, which are derived from the fractional analogue of the classical stress–strain equation for the elastic materials that involves the relaxation function of the power-law form, could robustly describe the observed power-law behaviors of the viscoelastic materials with numerous experimental demonstrations [8, 33, 40].

Euler-Bernoulli beam theory is applicable for long-slender elastic beams but is no longer suitable for thick beams, composite beams and beams under high frequency excitations. In contrast, the Timoshenko beam theory additionally considers the effects of rotary inertia and the shear deformation and has thus been widely used to characterize the mechanical behavior of the aforementioned beams. For instance, Fig. 1 compares the bending behavior of these two kinds of beams under deformation to illustrate the difference, which is characterized by the total angle ζ of rotation of the centroidal axis of beams. In the Timoshenko beam model $\zeta = \zeta_b + \zeta_s$ as presented in the left plot of Fig. 1 where ζ_b and ζ_s are due to bending and shearing, respectively, while the Euler-Bernoulli beam model only assumes $\zeta = \zeta_b$ as shown in the right plot of Fig. 1, see also §6.3 for numerical validation.

We consider the following fractional Timoshenko beam model [12, 28, 35, 41, 42, 48], which characterizes the mechanical responses of viscoelastic beams, thick beams, and beams under high-frequency excitations by properly taking shear force and rotational inertia into consideration

$$\begin{aligned} \rho A(x)\partial_t^2 w &= \partial_x\big(\kappa G A(x)\partial_t^\alpha\big(\partial_x w - \theta\big)\big) + q(x,t), \\ \rho I(x)\partial_t^2 \theta &= \partial_x\big(E I(x)\partial_x \partial_t^\alpha \theta\big) + \kappa G A(x)\partial_t^\alpha\big(\partial_x w - \theta\big). \end{aligned} \tag{1}$$

Here $(x,t) \in (0,l)\times(0,T]$ where l is the beam length, $w(x,t)$ and $\theta(x,t)$ are the transverse deflection and the angle of rotation of the cross section at x, $A(x)$ is the cross-sectional area, $q(x,t)$ is the external force, ρ is the mass density of the material, E is Young's elastic modulus for the beam, $I(x)$ is the rotational inertial, G is the shear modulus, and κ is the shear coefficient which is a dimensionless factor that depends on the shape of the cross-sectional area. The ∂_t^α with $0 < \alpha < 1$ refers to the Caputo fractional differential operator defined by [23, 34]

$$\partial_t^\alpha g(t) := {}_0I_t^{1-\alpha}\partial_t g(t), \quad {}_0I_t^\alpha g(t) := \frac{1}{\Gamma(\alpha)}\int_0^t \frac{g(s)}{(t-s)^{1-\alpha}}ds. \tag{2}$$

We note that the viscoelastic beams modeled by (1) are anticipated to exhibit solid elastic behavior when the fractional order $\alpha \to 0$, and to demonstrate viscous behavior due to the inherent viscoelastic damping mechanism with $\alpha \to 1$.

In this work we assume that the beam is clamped at both ends so the displacement w and the angle of rotation θ vanish at both ends, leading to the boundary conditions

$$w(0,t) = w(l,t) = 0, \quad \theta(0,t) = \theta(l,t) = 0, \quad t \in [0,T], \tag{3}$$

and we close system (1) by the initial conditions

$$\begin{aligned} w(x,0) = w_0(x), \quad \partial_t w(x,0) = \breve{w}_0(x), \quad x \in [0,l], \\ \theta(x,0) = \theta_0(x), \quad \partial_t \theta(x,0) = \breve{\theta}_0(x), \quad x \in [0,l]. \end{aligned} \tag{4}$$

After the model reformulation (cf. §3), each equation in model (1) takes the form of a parabolic integro-differential equation with a memory kernel, which has been extensively investigated in the literature [6, 13, 16, 18–20, 38, 44]. In [26], a parabolic integro-differential equation with either smooth or the power-function kernel $\beta(t) = t^{\alpha-1}$ for $0 < \alpha < 1$ modeling the viscoelasticity in shape-memory materials has been mathematically and numerically analyzed. Semi-discrete finite element approximations for parabolic integro-differential equations with integrable kernels have been proved in [21]. Optimal error estimates of the H^1-Galerkin mixed finite element methods for parabolic partial integral-differential equations arising from the materials with memory effects are established in [32]. In [46] the finite element approximation to a nonlinear hyperbolic integro-differential equation with L^1 convolution kernel is analyzed. To compensate for the singularity of the solutions at the initial time, quadrature methods [22, 27] and discontinuous Galerkin methods [30] on non-uniform temporal grids are applied to recover the optimal-order convergence rates. Convergence of finite element solutions of stochastic partial integro-differential equations driven by white noise has been analyzed in [11].

Compared with the extensive studies for a single parabolic integro-differential equation, there are much less investigations for numerical methods of model (1) due to, e.g. the coupling of the two equations and the lack of high-order regularity estimates of the solutions. To compensate for this gap, we derive high-order regularity results of the solutions to model (1) and then accordingly prove error estimates of the finite element scheme for the system (1) by technical derivations. The rest of the paper is organized as follows. In §2, we present preliminaries to be used subsequently. In §3, we prove high-order regularity of the solutions. In §4, we derive a fully-discrete finite element scheme for the fractional Timoshenko beam model and prove auxiliary estimates. In §5, we derive error estimates for the proposed scheme. Numerical experiments are carried out in §6 to substantiate the theoretical findings and to demonstrate the effectiveness of the fractional Timoshenko beam model in modeling the mechanical vibrations of different beams compared with its integer-order analogue and the integer-order and fractional Euler-Bernoulli beam models. We address concluding remarks in the last section.

2 Preliminaries

For $m \in \mathbb{N}$ (the set of nonnegative integers), $1 \le p \le \infty$, and $\mathcal{I} := (0,l)$ or $[0,T]$, let $C^m[0,T]$ be the Banach space of continuous functions with continuous derivatives up to order m on $[0,T]$. Let $L^p(\mathcal{I})$ be the Banach space of pth power Lebesgue integrable functions on $\mathcal{I}$ and $W^{m,p}(\mathcal{I})$ be the Sobolev space of functions with derivatives up to order m in $L^p(\mathcal{I})$.

Let $H^m(\mathcal{I}) = W^{m,2}(\mathcal{I})$ and $H_0^m(\mathcal{I})$ be its subspace with zero boundary conditions up to order $m-1$. All the spaces are equipped with standard norms [1].

For a Banach space $\mathcal{X}$, define $W^{m,p}(0,T;\mathcal{X})$ by [1, 10]

$$W^{m,p}(0,T;\mathcal{X}) := \left\{ g : \left\| \partial_t^k g(\cdot,t) \right\|_{\mathcal{X}} \in L^p(0,T), \ \ 0 \le k \le m \right\}$$

equipped with the norm

$$\|g\|_{W^{m,p}(0,T;\mathcal{X})} := \begin{cases} \left(\sum_{k=0}^{m} \int_0^T \left\| \partial_t^k g(\cdot,t) \right\|_{\mathcal{X}}^p dt \right)^{1/p}, & 1 \le p < \infty, \\ \max\limits_{0\le k\le m} \operatorname{ess\,sup}\limits_{t\in(0,T)} \left\| \partial_t^k g(\cdot,t) \right\|_{\mathcal{X}}, & p = \infty. \end{cases}$$

Through out this paper we shall use Q and Q_i to denote generic positive constants where Q may assume different values at different occurrences. We set $\|\cdot\| := \|\cdot\|_{L^2(\mathcal{I})}$ and abbreviate $W^{m,p}(0,T;\mathcal{X})$ as $W^{m,p}(\mathcal{X})$ for simplicity.

Lemma 1 [7, 9, 34, 37] *The left fractional integral operator ${}_0I_t^\beta$ and the right fractional integral operator*

$${}_tI_T^\beta g(t) := \frac{1}{\Gamma(\beta)} \int_t^T \frac{g(s)}{(s-t)^{1-\beta}} ds$$

are bounded linear operators in $L^2(0,T)$ with the semigroup properties

$${}_0I_t^{\beta_1}\, {}_0I_t^{\beta_2} v = {}_0I_t^{\beta_1+\beta_2} v, \ \ {}_tI_T^{\beta_1}\, {}_tI_T^{\beta_2} v = {}_tI_T^{\beta_1+\beta_2} v \ \ \forall t \in [0,T], \ \beta_1, \beta_2 > 0, \tag{5}$$

and they are adjoint operators in the sense that

$$\int_0^T ({}_0I_t^\beta w) v(t) dt = \int_0^T w(t) ({}_tI_T^\beta v) dt, \ \ w, v \in L^2(0,T), \ \ \beta > 0. \tag{6}$$

The operator ${}_0I_t^\beta$ with $0 < \beta < 1$ could commute with the differential operator ∂_t

$$\partial_t^{1-\beta} v = {}_0I_t^\beta \partial_t v = \partial_t\, {}_0I_t^\beta v, \quad \forall v \in W^{1,1}(0,T) \text{ with } v(0) = 0. \tag{7}$$

Lemma 2 [47, 48] *The following coercivity holds for $0 < \beta < 1/2$ if both sides of the equation exist for $\bar{t} \in [0,T]$*

$$\int_0^{\bar{t}} {}_0I_t^\beta g \cdot {}_tI_{\bar{t}}^\beta g \, dt \ge \cos(\beta\pi) \left\| {}_0I_t^\beta g \right\|_{L^2(0,\bar{t})}^2 = \cos(\beta\pi) \left\| {}_tI_{\bar{t}}^\beta g \right\|_{L^2(0,\bar{t})}^2 \tag{8}$$

Lemma 3 [45, Theorem 3.2] *Let $a \ge 0$ and $b > 0$ be constants and suppose that ϑ, $\iota \ge 0$ and $\vartheta + \iota < 1$. Suppose that $v \ge 0$ satisfies the inequality*

$$v(t) \le a + b \int_0^t (t-s)^{-\vartheta} s^{-\iota} v(s) ds, \ \text{for a.e. } t \in [0,T]. \tag{9}$$

We write $B_0 := B(1-\vartheta, 1-\iota)$. For $r > 0$, let $t_r := \left(\frac{r}{bB_0}\right)^{\frac{1}{1-\vartheta-\iota}}$ and let $r_0 := bB_0 T^{1-\vartheta-\iota}$ so that $t_r \le T$ for $r \le r_0$. Then, if $r \le r_0$ and also $r < 1$, we have

$$v(t) \le \frac{a}{1-r} \exp\left(\frac{b t_r^{-\vartheta}}{(1-r)(1-\iota)} t^{1-\iota} \right), \ \text{for a.e. } t \in [0,T]. \tag{10}$$

3 Regularity

For the convenience of the analysis, we use the substitution

$$u(x,t) := w(x,t) - w_0(x) - t\ \breve{w}_0(x), \quad \psi(x,t) := \theta(x,t) - \theta_0(x) - t\ \breve{\theta}_0(x) \tag{11}$$

to reformulate system (1) in terms of u and ψ as follows

$$\begin{aligned} \rho A(x)\partial_t^2 u &= \partial_x\big(\kappa G A(x)\partial_t^\alpha\big(\partial_x u - \psi\big)\big) + \tilde{q}(x,t), \\ \rho I(x)\partial_t^2 \psi &= \partial_x\big(E I(x)\partial_x \partial_t^\alpha \psi\big) + \kappa G A(x)\partial_t^\alpha\big(\partial_x u - \psi\big) + \tilde{p}(x,t) \end{aligned} \tag{12}$$

along with the homogenous initial and boundary conditions

$$u(0,t) = \psi(0,t) = u(l,t) = \psi(l,t) = 0, \quad t \in [0,T], \tag{13}$$

$$u(x,0) = \partial_t u(x,0) = \psi(x,0) = \partial_t \psi(x,0) = 0, \quad x \in [0,l]. \tag{14}$$

Here $\tilde{q}$ and $\tilde{p}$ are defined by

$$\begin{aligned} \tilde{q} &:= q + \kappa G \partial_x\big(A(x) I_t^{1-\alpha}\big(\partial_x \breve{w}_0 - \breve{\theta}_0\big)\big) \\ &= q + \frac{t^{1-\alpha}\kappa G \partial_x\big(A(x)\big(\partial_x \breve{w}_0 - \breve{\theta}_0\big)\big)}{\Gamma(2-\alpha)}, \\ \tilde{p} &:= E\partial_x\big(I(x)\partial_x\, {}_0I_t^{1-\alpha}\breve{\theta}_0\big) + \kappa G A(x)\, {}_0I_t^{1-\alpha}\big(\partial_x \breve{w}_0 - \breve{\theta}_0\big) \\ &= \frac{t^{1-\alpha}\big[E\partial_x\big(I(x)\partial_x \breve{\theta}_0\big) + \kappa G A(x)\big(\partial_x \breve{w}_0 - \breve{\theta}_0\big)\big]}{\Gamma(2-\alpha)}. \end{aligned} \tag{15}$$

Integrate equations (12) from 0 to t, apply the homogeneous initial conditions in (14) and use (7) to reach a coupled first-order system

$$\begin{aligned} \rho A(x)\partial_t u &= \kappa G \partial_x\big(A(x)\, {}_0I_t^{1-\alpha}\big(\partial_x u - \psi\big)\big) + f(x,t), \\ \rho I(x)\partial_t \psi &= E\partial_x\big(I(x)\, {}_0I_t^{1-\alpha}\partial_x \psi\big) + \kappa G A(x)\, {}_0I_t^{1-\alpha}\big(\partial_x u - \psi\big) + g(x,t), \end{aligned} \tag{16}$$

where $f := {}_0I_t^1 \tilde{q}$ and $g := {}_0I_t^1 \tilde{p}$. System (16) is closed with the boundary condition (13) and the initial condition

$$u(x,0) = 0, \quad \psi(x,0) = 0, \quad x \in [0,l]. \tag{17}$$

Note that the two homogeneous initial conditions on $\partial_t u(x,0)$ and $\partial_t \psi(x,0)$ in (14) can be deduced naturally from (16) by taking the limit $t \to 0^+$.

We cite the well-posedness and regularity of the problem (16)–(13)–(17) from [48].

Theorem 1 [48] *Suppose that* $\breve{w}_0, \breve{\theta}_0 \in H^2$, $q \in L^2(0,T;L^2)$ *and* $A, I \in H^1$ *with* $0 < A_* \le A(x), I(x) \le A^* < \infty$. *Then problem* (16)–(13)–(17) *has the unique solution* $u, \psi \in W^{1,\infty}(0,T;L^2) \cap L^2(0,T;H^1)$ *with*

$$\begin{aligned} &\|u\|_{W^{1,\infty}(0,T;L^2)} + \|u\|_{L^2(0,T;H^1)} + \|\psi\|_{W^{1,\infty}(0,T;L^2)} + \|\psi\|_{L^2(0,T;H^1)} \\ &\quad \le Q\big(\|f\|_{H^1(0,T;L^2)} + \|g\|_{H^1(0,T;L^2)}\big) \le Q\big(\|q\|_{L^2(0,T;L^2)} + \|\breve{w}_0\|_{H^2} + \|\breve{\theta}_0\|_{H^2}\big) \end{aligned}$$

with $Q = Q(\rho, A_*, A^*, \|A\|_{H^1}, \|I\|_{H^1}, \kappa, G, E, \alpha, T)$.

If further $q \in H^1(0,T;L^2)$, *then* $u, \psi \in W^{2,\infty}(0,T;L^2) \cap L^2(0,T;H^2)$ *with*

$$\begin{aligned} &\|u\|_{W^{2,\infty}(0,T;L^2)} + \|\psi\|_{W^{2,\infty}(0,T;L^2)} + \|u\|_{L^2(0,T;H^2)} + \|\psi\|_{L^2(0,T;H^2)} \\ &\quad \le Q\big(\|\breve{w}_0\|_{H^2} + \|\breve{\theta}_0\|_{H^2} + \|q\|_{H^1(0,T;L^2)}\big). \end{aligned}$$

Here the constant $Q = Q(\rho, A_*, A^*, \|A\|_{H^1}, \|I\|_{H^1}, \kappa, G, E, \alpha, T)$.

We then prove the regularity of the solutions u and ψ to the problem (16)–(13)–(17) in the following theorem to support the subsequent numerical analysis.

Theorem 2 *If* $\breve{w}_0, \breve{\theta}_0 \in H^2$, $q \in H^2(0,T;L^2)$ *with* $\partial_x q(x,0) \in L^2$, $A, I \in W^{1,\infty}$ *with* $A_* \le A(x), I(x) \le A^*$, *then* $u, \psi \in W^{1,\infty}(0,T;H^2)$ *with the estimates for some constant* $Q = Q(\rho, A_*, A^*, \|A\|_{W^{1,\infty}}, \|I\|_{W^{1,\infty}}, \kappa, G, E, \alpha, T)$

$$\begin{aligned}&\|u\|_{W^{1,\infty}(0,T;H^2)} + \|\psi\|_{W^{1,\infty}(0,T;H^2)}\\ &\quad\le Q\big(\|\breve{w}_0\|_{H^2} + \|\breve{\theta}_0\|_{H^2} + \|q\|_{H^2(0,T;L^2)} + \|\partial_x q(x,0)\|\big).\end{aligned}$$

Proof We deduce from (14) that $\partial_t\partial_x u(x,0) = \partial_t\partial_x^2 u(x,0) = \partial_t\partial_x\psi(x,0) = \partial_t\partial_x^2\psi(x,0) = 0$, and we apply them to pass the limit $t \to 0^+$ in (12) to get

$$\begin{aligned}&\lim_{t\to 0^+} \partial_x\big(\kappa G A(x)\partial_t^\alpha\big(\partial_x u - \psi\big)\big) = 0,\\ &\lim_{t\to 0^+} E\partial_x\big(I(x)\partial_t^\alpha\partial_x\psi\big) + \kappa G A(x)\partial_t^\alpha\big(\partial_x u - \psi\big) = 0,\end{aligned}$$

that is, $\rho A\partial_t^2 u(x,0) = q(x,0)$ and $\rho I\partial_t^2\psi(x,0) = 0$, which imply $\partial_t^2\partial_x u(x,0) = \partial_x\big(q(x,0)/\rho A\big)$ and $\partial_t^2\partial_x\psi(\cdot,0) = 0$.

We then apply the operator $\partial_t\, {}_0I_t^\alpha\partial_t^2$ to both sides of the equations in (16), integrate the resulting equations over $(0,l)$ multiplied by ${}_0I_t^\alpha\partial_t^3 u$ and ${}_0I_t^\alpha\partial_t^3\psi$, respectively, and use the properties in Lemma 1, as well as the derivations like

$$\begin{aligned}\partial_t\, {}_0I_t^\alpha\partial_t^2\, {}_0I_t^{1-\alpha}\partial_x u(\cdot,t) &= \partial_t\, {}_0I_t^\alpha\partial_t\, {}_0I_t^{1-\alpha}\partial_t\partial_x u(\cdot,t)\\ &= \partial_t\partial_t\, {}_0I_t^\alpha\, {}_0I_t^{1-\alpha}\partial_t\partial_x u(\cdot,t) = \partial_t^2\partial_x u(\cdot,t)\\ &= {}_0I_t^1\partial_t^3\partial_x u(\cdot,t) + \partial_t^2\partial_x u(\cdot,0) = {}_0I_t^{1-\alpha}\, {}_0I_t^\alpha\partial_t^3\partial_x u(\cdot,t) + \partial_t^2\partial_x u(\cdot,0)\end{aligned}$$

to get

$$\begin{aligned}&\rho\big(A\partial_t\, {}_0I_t^\alpha\partial_t^3 u, {}_0I_t^\alpha\partial_t^3 u\big) + \kappa G\big(A\, {}_0I_t^{1-\alpha}\, {}_0I_t^\alpha\partial_t^3\partial_x u, {}_0I_t^\alpha\partial_t^3\partial_x u\big)\\ &\quad= \kappa G\big(A\, {}_0I_t^{1-\alpha}\, {}_0I_t^\alpha\partial_t^3\psi, {}_0I_t^\alpha\partial_t^3\partial_x u\big) + \big(f_*, {}_0I_t^\alpha\partial_t^3 u\big),\\ &\rho\big(I\partial_t\, {}_0I_t^\alpha\partial_t^3\psi, {}_0I_t^\alpha\partial_t^3\psi\big) + E\big(I\, {}_0I_t^{1-\alpha}\, {}_0I_t^\alpha\partial_t^3\partial_x\psi, {}_0I_t^\alpha\partial_t^3\partial_x\psi\big)\\ &\quad+\kappa G\big(A\, {}_0I_t^{1-\alpha}\, {}_0I_t^\alpha\partial_t^3\psi, {}_0I_t^\alpha\partial_t^3\psi\big)\\ &\quad= \kappa G\big(A\, {}_0I_t^{1-\alpha}\, {}_0I_t^\alpha\partial_t^3\partial_x u, {}_0I_t^\alpha\partial_t^3\psi\big) + \big(g_*, {}_0I_t^\alpha\partial_t^3\psi\big),\end{aligned}\tag{18}$$

with $f_* = \partial_t\, {}_0I_t^\alpha\partial_t q - \kappa GA\partial_x\big(\frac{q(x,0)}{\rho A}\big)$ and $g_* = \partial_t\, {}_0I_t^\alpha\partial_t^2 g = 0$. We integrate these two equations from 0 to t and apply Lemmas 1–2 as well as

$$\begin{aligned}\int_0^t \rho\big(A\partial_s\, {}_0I_s^\alpha\partial_s^3 u, {}_0I_s^\alpha\partial_s^3 u\big)ds &= \frac{1}{2}\int_0^t \partial_s\|\sqrt{\rho A}\, {}_0I_s^\alpha\partial_s^3 u\|^2 ds\\ &= \frac{1}{2}\|\sqrt{\rho A}\, {}_0I_t^\alpha\partial_t^3 u\|^2 - \frac{1}{2}\|\sqrt{\rho A}\, {}_0I_s^\alpha\partial_s^3 u\|^2\Big|_{s=0}\end{aligned}$$

to reach at a lower bound estimate for the left-hand side of the first equation in (18)

$$\begin{aligned}&\int_0^t \rho\big(A\partial_s\, {}_0I_s^\alpha\partial_s^3 u, {}_0I_s^\alpha\partial_s^3 u\big) + \kappa G\int_0^t \big(A\, {}_0I_s^{1-\alpha}\, {}_0I_s^\alpha\partial_s^3\partial_x u, {}_0I_s^\alpha\partial_s^3\partial_x u\big)ds\\ &\ge \frac{\rho A_*}{2}\|{}_0I_t^\alpha\partial_t^3 u\|^2 - \frac{\rho A^*}{2}\|{}_0I_s^\alpha\partial_s^3 u\|^2\Big|_{s=0}\\ &\quad+\kappa GA_*\cos\left(\frac{(1-\alpha)\pi}{2}\right)\big\|{}_0I_t^{\frac{1-\alpha}{2}}\, {}_0I_t^\alpha\partial_t^3\partial_x u\big\|^2_{L^2(0,t;L^2)}.\end{aligned}\tag{19}$$

We then employ Cauchy's inequality and Lemma 2 to bound the right-hand side terms of the first equation in (18) by

$$\begin{aligned}
&\int_0^t \kappa G\big(A\,{}_0I_s^{1-\alpha}\,{}_0I_s^{\alpha}\partial_s^3\psi,\,{}_0I_s^{\alpha}\partial_s^3\partial_x u\big)+\big(f_*,\,{}_0I_s^{\alpha}\partial_s^3 u\big)ds\\
&\quad\le \frac{\kappa G A_*}{4}\cos\left(\frac{(1-\alpha)\pi}{2}\right)\big\|{}_0I_t^{\frac{1-\alpha}{2}}\,{}_0I_t^{\alpha}\partial_t^3\partial_x u\big\|^2_{L^2(0,t;L^2)}\\
&\qquad+Q\big\|{}_0I_t^{\frac{1-\alpha}{2}}\,{}_0I_t^{\alpha}\partial_t^3\psi\big\|^2_{L^2(0,t;L^2)}+\int_0^t\big\|f_*(\cdot,s)\big\|\big\|{}_0I_s^{\alpha}\partial_s^3 u(\cdot,s)\big\|ds.
\end{aligned}\tag{20}$$

We incorporate (18) with the estimates (19)–(20) and apply the mapping property $\big\|{}_0I_t^{\frac{1-\alpha}{2}}\,{}_0I_t^{\alpha}\partial_t^3\psi\big\|_{L^2(0,t;L^2)}\le Q\big\|{}_0I_t^{\alpha}\partial_t^3\psi\big\|_{L^2(0,t;L^2)}$ to obtain

$$\begin{aligned}
&\frac{\rho A_*}{2}\big\|{}_0I_t^{\alpha}\partial_t^3 u\big\|^2+\frac{3}{4}\cos\left(\frac{(1-\alpha)\pi}{2}\right)\kappa G A_*\big\|{}_0I_t^{\frac{1-\alpha}{2}}\,{}_0I_t^{\alpha}\partial_t^3\partial_x u\big\|^2_{L^2(0,t;L^2)}\\
&\le\frac{\rho A^*}{2}\|{}_0I_s^{\alpha}\partial_s^3 u\|^2\Big|_{s=0}+Q\big\|{}_0I_t^{\alpha}\partial_t^3\psi\big\|^2_{L^2(0,t;L^2)}\\
&\quad+\int_0^t\big\|f_*(\cdot,s)\big\|\big\|{}_0I_s^{\alpha}\partial_s^3 u(\cdot,s)\big\|ds.
\end{aligned}\tag{21}$$

A similar inequality as (21) could be derived in an analogous manner from the second equation of (18), and we add these two inequalities to get

$$\begin{aligned}
&\big\|{}_0I_t^{\alpha}\partial_t^3 u\big\|^2+\big\|{}_0I_t^{\alpha}\partial_t^3\psi\big\|^2+\big(\big\|{}_0I_t^{\frac{1-\alpha}{2}}\,{}_0I_t^{\alpha}\partial_t^3\partial_x u\big\|^2_{L^2(0,t;L^2)}\\
&\quad+\big\|{}_0I_t^{\frac{1-\alpha}{2}}\,{}_0I_t^{\alpha}\partial_t^3\partial_x\psi\big\|^2_{L^2(0,t;L^2)}+\big\|{}_0I_t^{\frac{1-\alpha}{2}}\,{}_0I_t^{\alpha}\partial_t^3\psi\big\|^2_{L^2(0,t;L^2)}\big)\\
&\le Q\big(\|{}_0I_s^{\alpha}\partial_s^3 u\|^2+\|{}_0I_s^{\alpha}\partial_s^3\psi\|^2\big)\Big|_{s=0}+Q\|{}_0I_t^{\alpha}\partial_t^3\psi\|^2_{L^2(0,t;L^2)}\\
&\quad+Q\int_0^t\big\|f_*(\cdot,s)\big\|\big\|{}_0I_s^{\alpha}\partial_s^3 u(\cdot,s)\big\|ds.
\end{aligned}\tag{22}$$

To estimate the first two right-hand side terms of (22), we apply the operator ${}_0I_t^{\alpha}\partial_t$ on both sides of the equations in (12) and pass the limit $t\to 0^+$ in the resulting equations to get $\rho A(x)\,{}_0I_t^{\alpha}\partial_t^3 u|_{t=0}={}_0I_t^{\alpha}\partial_t\tilde{q}(x,t)|_{t=0}$ and $\rho I(x)\,{}_0I_t^{\alpha}\partial_t^3\psi|_{t=0}={}_0I_t^{\alpha}\partial_t\tilde{p}(x,t)|_{t=0}$. We then apply the norm $\|\cdot\|_{L^2(0,l)}$ on both sides of them and employ (15) to deduce

$$\begin{aligned}
\big(\|{}_0I_t^{\alpha}\partial_t^3 u\|^2+\|{}_0I_t^{\alpha}\partial_t^3\psi\|^2\big)\big|_{t=0}&\le Q(\|{}_0I_t^{\alpha}\partial_t\tilde{q}(\cdot,t)\|+\|{}_0I_t^{\alpha}\partial_t\tilde{p}(\cdot,t)\|\big)\big|_{t=0}\\
&\le Q(\|{}_0I_t^{\alpha}\partial_t q(\cdot,t)\|\big|_{t=0}+\|\breve{w}_0\|_{H^2}+\|\breve{\theta}_0\|_{H^2})\le Q(\|\breve{w}_0\|_{H^2}+\|\breve{\theta}_0\|_{H^2})
\end{aligned}\tag{23}$$

for $Q=Q(\rho,A_*,A^*,\|A\|_{W^{1,\infty}},\|I\|_{W^{1,\infty}},\kappa,G,E,\alpha,T)$. To estimate f_*, we apply integration by parts to obtain

$$\partial_t\,{}_0I_t^{\alpha}\partial_t q=\partial_t\int_0^t\frac{\partial_s q(x,s)ds}{\Gamma(\alpha)(t-s)^{1-\alpha}}=\frac{t^{\alpha-1}}{\Gamma(\alpha)}\partial_t q(x,0)+{}_0I_t^{\alpha}\partial_t^2 q(x,t).\tag{24}$$

We follow the procedures in [48, Theorem V.1] to employ the estimate (24) together with the Sobolev embedding $H^2(0,T)\hookrightarrow C^1[0,T]$ and $1=(t-s)^{-\varepsilon}(t-s)^{\varepsilon}\le Q(t-s)^{-\varepsilon}$ for $0<\varepsilon\ll 1$ to bound the last right-hand side term of (22)

$$\begin{aligned}
&\|f_*(\cdot,s)\|\le Qs^{\alpha-1}\big\|\partial_s q(\cdot,0)\big\|+Q\big(\big\|{}_0I_s^{\alpha}\partial_s^2 q(\cdot,s)\big\|+\|\partial_x q(\cdot,0)\|+\|q(\cdot,0)\|\big),\\
&\int_0^t\big\|f_*(\cdot,s)\big\|\big\|{}_0I_s^{\alpha}\partial_s^3 u(\cdot,s)\big\|ds\quad\le Q\int_0^t s^{\alpha-1}(t-s)^{-\varepsilon}\big\|{}_0I_s^{\alpha}\partial_s^3 u(\cdot,s)\big\|^2 ds\\
&\qquad+Q\big(\|q\|^2_{H^2(0,T;L^2)}+\big\|{}_0I_s^{\alpha}\partial_s^3 u\big\|^2_{L^2(0,t;L^2)}+\|\partial_x q(\cdot,0)\|^2\big).
\end{aligned}\tag{25}$$

We drop the last three terms on the left-hand side of (22) and invoke the estimates (23)–(25) to get

$$\begin{aligned}\left\|{}_0I_t^{\alpha}\partial_t^3u(\cdot,t)\right\|^2+\left\|{}_0I_t^{\alpha}\partial_t^3\psi(\cdot,t)\right\|^2\le Q\int_0^t(t-s)^{-\varepsilon}s^{\alpha-1}\left\|{}_0I_s^{\alpha}\partial_s^3u(\cdot,s)\right\|^2ds\\ +Q\left(\left\|{}_0I_s^{\alpha}\partial_s^3u\right\|^2_{L^2(0,t;L^2)}+\left\|{}_0I_s^{\alpha}\partial_s^3\psi\right\|^2_{L^2(0,t;L^2)}\right)\\ +Q\left(\|q\|^2_{H^2(L^2)}+\|\breve{w}_0\|^2_{H^2}+\|\breve{\theta}_0\|^2_{H^2}+\|\partial_xq(\cdot,0)\|^2\right).\end{aligned}\tag{26}$$

Then we apply the Gronwall inequality in Lemma 3 to conclude

$$\left\|{}_0I_t^{\alpha}\partial_t^3u\right\|+\left\|{}_0I_t^{\alpha}\partial_t^3\psi\right\|\le Q(\|q\|_{H^2(L^2)}+\|\breve{w}_0\|_{H^2}+\|\breve{\theta}_0\|_{H^2}+\|\partial_xq(\cdot,0)\|).\tag{27}$$

Similar to the derivation of (18), we apply the operator $\partial_t^2\,{}_0I_t^{\alpha}$ to (16), integrate the resulting equations multiplied by $\phi\in H_0^1(0,l)$ and utilize (7), the homogeneous initial conditions (14) and $g(x,0)=g'(x,0)=0$ to find

$$\begin{aligned}\kappa G\left(A\partial_t\partial_xu,\partial_x\phi\right)&=-\rho\left(A\partial_t\,{}_0I_t^{\alpha}\partial_t^2u,\phi\right)+\kappa G\left(A\partial_t\psi,\partial_x\phi\right)+\left(\partial_t^2\,{}_0I_t^{\alpha}f,\phi\right),\\ E\left(I\partial_t\partial_x\psi,\partial_x\phi\right)&=-\rho\left(I\partial_t\,{}_0I_t^{\alpha}\partial_t^2\psi,\phi\right)-\kappa G\left(A\partial_t\psi,\phi\right)\\ &\quad+\kappa G\left(A\partial_t\partial_xu,\phi\right)+\left({}_0I_t^{\alpha}\partial_t^2g,\phi\right).\end{aligned}\tag{28}$$

To rewrite the right-hand side terms of (28), we apply $f(x,0)=0$, $\rho A\partial_t^2u(x,0)=q(x,0)$ and the integration by parts to obtain for $t\in(0,T]$

$$\begin{aligned}\partial_t\,{}_0I_t^{\alpha}\partial_t^2u&={}_0I_t^{\alpha}\partial_t^3u+\frac{t^{\alpha-1}}{\Gamma(\alpha)}\partial_t^2u(x,0)={}_0I_t^{\alpha}\partial_t^3u+\frac{t^{\alpha-1}}{\Gamma(\alpha)}\frac{q(x,0)}{\rho A},\\ \partial_t^2\,{}_0I_t^{\alpha}f&=\partial_t\,{}_0I_t^{\alpha}\partial_tf={}_0I_t^{\alpha}\partial_t^2f+\frac{t^{\alpha-1}}{\Gamma(\alpha)}\partial_tf(x,0)={}_0I_t^{\alpha}\partial_t^2f+\frac{t^{\alpha-1}}{\Gamma(\alpha)}q(x,0),\end{aligned}$$

which give

$$(-\rho A\partial_t\,{}_0I_t^{\alpha}\partial_t^2u+\partial_t^2\,{}_0I_t^{\alpha}f,\phi)=-\rho(A\,{}_0I_t^{\alpha}\partial_t^3u,\phi)+({}_0I_t^{\alpha}\partial_t^2f,\phi).$$

Similarly we use $\rho I\partial_t^2\psi(x,0)=0$ to get $\partial_t\,{}_0I_t^{\alpha}\partial_t^2\psi={}_0I_t^{\alpha}\partial_t^3\psi$. We incorporate these relations in (28) to obtain

$$\begin{aligned}\kappa G\left(A\partial_t\partial_xu,\partial_x\phi\right)&=-\rho\left(A\,{}_0I_t^{\alpha}\partial_t^3u,\phi\right)+\kappa G\left(A\partial_t\psi,\partial_x\phi\right)+\left({}_0I_t^{\alpha}\partial_t^2f,\phi\right),\\ E\left(I\partial_t\partial_x\psi,\partial_x\phi\right)&=-\rho\left(I\,{}_0I_t^{\alpha}\partial_t^3\psi,\phi\right)-\kappa G\left(A\partial_t\psi,\phi\right)\\ &\quad+\kappa G\left(A\partial_t\partial_xu,\phi\right)+\left({}_0I_t^{\alpha}\partial_t^2g,\phi\right).\end{aligned}\tag{29}$$

We set $\phi=\partial_t^2u$ and $\phi=\partial_t^2\psi$ in the first and second equations of (29), respectively, and integrate the resulting equations from 0 to t to reach

$$\begin{aligned}\left\|\partial_t\partial_xu(\cdot,t)\right\|^2&\le Q\|\partial_s\partial_xu(\cdot,s)\|^2\big|_{s=0}\\ &\quad+Q\int_0^t(\left\|\partial_s^2u(\cdot,s)\right\|^2+\left\|\partial_s\partial_x\psi(\cdot,s)\right\|^2+\left\|\partial_s\psi(\cdot,s)\right\|^2)ds\\ &\quad+Q\int_0^t\left(\left\|A\,{}_0I_s^{\alpha}\partial_s^3u(\cdot,s)\right\|+\left\|{}_0I_s^{\alpha}\partial_s^2f(\cdot,s)\right\|\right)\left\|\partial_s^2u(\cdot,s)\right\|ds,\\ \left\|\partial_t\partial_x\psi(\cdot,t)\right\|^2&\le Q\|\partial_s\partial_x\psi(\cdot,s)\|^2\big|_{s=0}+Q\int_0^t\left\|I\,{}_0I_s^{\alpha}\partial_s^3\psi(\cdot,s)\right\|\left\|\partial_s^2\psi(\cdot,s)\right\|ds\\ &\quad+Q\int_0^t\left\|\partial_s^2\psi(\cdot,s)\right\|^2+\left\|\partial_s\partial_xu(\cdot,s)\right\|^2+\left\|\partial_s\psi(\cdot,s)\right\|^2+\left\|{}_0I_s^{\alpha}\partial_s^2g\right\|^2ds.\end{aligned}\tag{30}$$

The two initial value terms on the right-hand side of (30) could be evaluated directly from the initial conditions in (14) by $\partial_t\partial_xu|_{t=0}=\partial_x\partial_tu(x,0)=0$ and $\partial_t\partial_x\psi|_{t=0}=\partial_x\partial_t\psi(x,0)=0$.

We follow the preceding procedures in (25) and incorporate (27) and Theorem 1 with (15) to bound the terms on the right-hand side of (30) by

$$\begin{aligned}
&\left\|{}_0I_s^{\alpha}\partial_s^2 f(\cdot,s)\right\| \le \left\|{}_0I_s^{\alpha}\partial_s q(\cdot,s)\right\| + Q(\|\check{w}_0\|_{H^2} + \|\check{\theta}_0\|_{H^1}),\\
&\int_0^t \left(\left\|A\,{}_0I_s^{\alpha}\partial_s^3 u(\cdot,s)\right\| + \left\|{}_0I_s^{\alpha}\partial_s^2 f(\cdot,s)\right\|\right)\left\|\partial_s^2 u(\cdot,s)\right\| ds\\
&\qquad + \int_0^t \left\|I\,{}_0I_s^{\alpha}\partial_s^3\psi(\cdot,s)\right\|\left\|\partial_s^2\psi(\cdot,s)\right\| ds\\
&\qquad \le Q\big(\|q\|^2_{H^2(L^2)} + \|\check{w}_0\|^2_{H^2} + \|\check{\theta}_0\|^2_{H^2} + \|\partial_x q(\cdot,0)\|^2\big).
\end{aligned} \tag{31}$$

We sum the two inequalities in (30) and invoke the preceding estimates to obtain for $t \in [0, T]$

$$\begin{aligned}
\left\|\partial_t\partial_x u(\cdot,t)\right\|^2 + \left\|\partial_t\partial_x\psi(\cdot,t)\right\|^2 &\le Q\int_0^t \left\|\partial_s\partial_x u(\cdot,s)\right\|^2 + \left\|\partial_s\partial_x\psi(\cdot,s)\right\|^2 ds\\
&+ Q(\|q\|^2_{H^2(L^2)} + \|\check{w}_0\|^2_{H^2} + \|\check{\theta}_0\|^2_{H^2} + \|\partial_x q(\cdot,0)\|^2).
\end{aligned} \tag{32}$$

Then an application of the Gronwall's inequality gives

$$\begin{aligned}
&\left\|\partial_t\partial_x u(\cdot,t)\right\| + \left\|\partial_t\partial_x\psi(\cdot,t)\right\|\\
&\qquad \le Q\big(\|q\|_{H^2(L^2)} + \|\check{w}_0\|_{H^2} + \|\check{\theta}_0\|_{H^2} + \|\partial_x q(\cdot,0)\|\big).
\end{aligned} \tag{33}$$

Finally, we apply the elliptic regularity theory [10] to (29) to get

$$\begin{aligned}
\left\|\partial_t u(\cdot,t)\right\|_{H^2} &\le Q\big(\left\|{}_0I_t^{\alpha}\partial_t^3 u(\cdot,t)\right\| + \left\|\partial_t\partial_x\psi(\cdot,t)\right\| + \left\|\partial_t\psi(\cdot,t)\right\| + \left\|{}_0I_t^{\alpha}\partial_t^2 f(\cdot,t)\right\|\big),\\
\left\|\partial_t\psi(\cdot,t)\right\|_{H^2} &\le Q\big(\left\|{}_0I_t^{\alpha}\partial_t^3\psi(\cdot,t)\right\| + \left\|\partial_t\psi(\cdot,t)\right\| + \left\|\partial_t\partial_x u(\cdot,t)\right\| + \left\|{}_0I_t^{\alpha}\partial_t^2 g(\cdot,t)\right\|\big),
\end{aligned}$$

and we incorporate the estimates (33), (27), (31), Theorem 1 and the Sobolev embedding $H^2(0, T) \hookrightarrow C^1[0, T]$ to obtain

$$\begin{aligned}
&\left\|\partial_t u(\cdot,t)\right\|_{H^2} + \left\|\partial_t\psi(\cdot,t)\right\|_{H^2}\\
&\quad \le Q\big(\|q\|_{H^2(L^2)} + \|q\|_{C^1(L^2)} + \|\check{w}_0\|_{H^2} + \|\check{\theta}_0\|_{H^2} + \|\partial_x q(\cdot,0)\|\big)\\
&\quad \le Q\big(\|q\|_{H^2(L^2)} + \|\check{w}_0\|_{H^2} + \|\check{\theta}_0\|_{H^2} + \|\partial_x q(\cdot,0)\|\big).
\end{aligned} \tag{34}$$

We incorporate (34) with $\|u(\cdot,0)\|_{H^2} = \|\psi(\cdot,0)\|_{H^2} = 0$ derived from (17) to conclude that

$$\begin{aligned}
\|u(\cdot,t)\|_{H^2} + \|\psi(\cdot,t)\|_{H^2} &\le \int_0^t \left\|\partial_s u(\cdot,s)\right\|_{H^2} + \left\|\partial_s\psi(\cdot,s)\right\|_{H^2} ds\\
&\le Q\big(\|q\|_{H^2(L^2)} + \|\check{w}_0\|_{H^2} + \|\check{\theta}_0\|_{H^2} + \|\partial_x q(\cdot,0)\|\big),
\end{aligned}$$

which completes the proof of this theorem. □

4 Numerical Scheme for Problem (16)

Let $t_n := n\tau$ for $n = 0, 1, \ldots, N$ with $\tau := T/N$ be a uniform partition on $[0, T]$, $u_n := u(x, t_n)$, $\psi_n := \psi(x, t_n)$, $f_n := f(x, t_n)$, $g_n := g(x, t_n)$ and $\beta(t) := t^{-\alpha}/\Gamma(1-\alpha)$. Then we introduce the discrete-in-time spaces $\hat{L}^1(0, t_n; L^2)$, $\hat{L}^2(0, t_n; L^2)$ and $\hat{L}^\infty(0, t_n; L^2)$ equipped with the norms for $v = \{v_j\}_{j=1}^N$ with $v_j \in L^2(0, l)$

$$\|v\|_{\hat{L}^p(0,t_n;L^2)} := \Big(\tau\sum_{j=1}^{n}\|v_j\|^p\Big)^{\frac{1}{p}}, \quad p = 1, 2; \quad \|v\|_{\hat{L}^\infty(0,t_n;L^2)} := \max_{1\le j\le n}\|v_j\|.$$

We perform temporal discretizations for $\partial_t u$ and ${}_0I_t^{1-\alpha}\psi$ at $t = t_n$ for illustration

$$\begin{aligned}
\partial_t u(x,t_n) &= \delta_\tau u_n + E_{u,n} := \frac{u_n - u_{n-1}}{\tau} + \frac{1}{\tau}\int_{t_{n-1}}^{t_n} u_{tt}(x,t)(t-t_{n-1})dt,\\
{}_0I_t^{1-\alpha}\psi(x,t_n) &= \sum_{j=1}^{n}\int_{t_{j-1}}^{t_j}\beta(t_n-s)\psi(x,s)ds := I_\tau^{1-\alpha}\psi_n + R_{\psi,n}.
\end{aligned} \tag{35}$$

Here $I_\tau^{1-\alpha}\psi_n$ and $R_{\psi,n}$ are defined by [26, 27]

$$\begin{aligned}
I_\tau^{1-\alpha}\psi_n &= \sum_{j=1}^{n}\int_{t_{j-1}}^{t_j}\beta(t_n-s)L_1\psi(\cdot,s)ds\\
&= \frac{1}{\tau}\sum_{j=1}^{n}\int_{t_{j-1}}^{t_j}\beta(t_n-s)\left[(t_j-s)\psi_{j-1}+(s-t_{j-1})\psi_j\right]ds := \sum_{j=0}^{n}c_{n,j}\psi_j,\\
R_{\psi,n} &= \sum_{j=1}^{n}\int_{t_{j-1}}^{t_j}\beta(t_n-s)(I-L_1)\psi(\cdot,s)ds,
\end{aligned} \tag{36}$$

where the coefficients $c_{n,j}$ for $0 \le j \le n \le N$ are defined by

$$\begin{aligned}
c_{n,0} &= \frac{1}{\tau}\int_0^\tau \beta(t_n-s)(\tau-s)ds,\\
c_{n,j} &= \frac{1}{\tau}\Bigg[\int_{t_{j-1}}^{t_j}\beta(t_n-s)(s-t_{j-1})ds\\
&\quad + \int_{t_j}^{t_{j+1}}\beta(t_n-s)(t_{j+1}-s)ds\Bigg], \quad 1 \le j \le n-1,\\
c_{n,n} &= \frac{1}{\tau}\int_{t_{n-1}}^{t_n}\beta(t_n-s)(s-t_{n-1})ds.
\end{aligned} \tag{37}$$

The L_1 refers to the temporal piecewise linear interpolation operator with respect to the partition $\{t_j\}_{j=1}^N$ and the corresponding error on $[t_{j-1}, t_j]$ could be expanded as

$$v(s) - L_1 v(s) = \int_{t_{j-1}}^{t_j} G_j(\theta;s)\frac{dv(\theta)}{d\theta}d\theta, \quad s \in [t_{j-1}, t_j] \tag{38}$$

where $G_j(\theta;s) := (t_j - s)/\tau$ for $\theta \in [t_{j-1}, s]$ or $-(s-t_{j-1})/\tau$ for $\theta \in [s, t_j]$.

The remaining terms $\partial_t\psi, {}_0I_t^{1-\alpha}\partial_x u, {}_0I_t^{1-\alpha}\partial_x\big(A\partial_x u\big), {}_0I_t^{1-\alpha}\partial_x\big(A\psi\big)$ and ${}_0I_t^{1-\alpha}\partial_x\big(I\partial_x\psi\big)$ could be discretized similarly at $t = t_n$ by $\delta_\tau\psi_n$, $I_\tau^{1-\alpha}\partial_x u_n$, $I_\tau^{1-\alpha}\partial_x\big(A\partial_x u_n\big)$, $I_\tau^{1-\alpha}\partial_x\big(A\psi_n\big)$ and $I_\tau^{1-\alpha}\partial_x\big(I\partial_x\psi_n\big)$ with truncation errors $E_{\psi,n}$, $R_{\partial_x u,n}$, $R_{\partial_x(A\partial_x u),n}$, $R_{\partial_x(A\psi),n}$ and $R_{\partial_x(I\partial_x\psi),n}$, respectively. We plug these discretizations into (16) and integrate the resulting equations multiplied by any $\chi \in H_0^1(0,l)$ to get a weak formulation for problem (16) for $n = 1, 2, \cdots, N$:

$$\begin{aligned}
&\rho\big(A\delta_\tau u_n, \chi\big) + \kappa G\big(AI_\tau^{1-\alpha}\partial_x u_n, \partial_x\chi\big)\\
&\quad = \kappa G\big(AI_\tau^{1-\alpha}\psi_n, \partial_x\chi\big) + \big(f_n, \chi\big) + \big(\kappa G R_{\partial_x(A\partial_x u - A\psi),n} - \rho A E_{u,n}, \chi\big),\\
&\rho\big(I\delta_\tau\psi_n, \chi\big) + E\big(I\, I_\tau^{1-\alpha}\partial_x\psi_n, \partial_x\chi\big) + \kappa G\big(AI_\tau^{1-\alpha}\psi_n, \chi\big)\\
&\quad = \kappa G\big(AI_\tau^{1-\alpha}\partial_x u_n, \chi\big) + \big(g_n, \chi\big) + \big(E R_{\partial_x(I\partial_x\psi),n} + \kappa G R_{A(\partial_x u - \psi),n} - \rho I E_{\psi,n}, \chi\big).
\end{aligned}$$

To derive a fully-discrete finite element scheme, let S_h be the space of continuous and piecewise linear functions on $[0, l]$ with respect to its quasi-uniform partition with the mesh

diameter h. It is known that the Ritz projections $\Pi_A : H_0^1(0,l) \to S_h$ and $\Pi_I : H_0^1(0,l) \to S_h$ defined by [43]

$$\big(A\partial_x \Pi_A v, \partial_x \chi\big) = \big(A\partial_x v, \partial_x \chi\big), \ \big(I\partial_x \Pi_I v, \partial_x \chi\big) = \big(I\partial_x v, \partial_x \chi\big), \ \forall \chi \in S_h \tag{39}$$

have the approximation properties for any $v \in H^2(0,l) \cap H_0^1(0,l)$ [43]

$$\|v - \Pi_A v\| \le Qh^2 \|v\|_{H^2}, \quad \|v - \Pi_I v\| \le Qh^2 \|v\|_{H^2}. \tag{40}$$

We then drop the local truncation errors in the weak formulation to arrive at the fully-discrete finite element scheme of (16): find $U_n, \Psi_n \in S_h$ with $U_0 := \Pi_A u_0 = 0$ and $\Psi_0 := \Pi_I \psi_0 = 0$ such that for $1 \le n \le N$ and $\chi \in S_h$

$$\begin{aligned} &\rho\big(A\delta_\tau U_n, \chi\big) + \kappa G\big(AI_\tau^{1-\alpha}\partial_x U_n, \partial_x \chi\big) = \kappa G\big(AI_\tau^{1-\alpha}\Psi_n, \partial_x \chi\big) + \big(f_n, \chi\big), \\ &\rho\big(I\delta_\tau \Psi_n, \chi\big) + E\big(I\, I_\tau^{1-\alpha}\partial_x \Psi_n, \partial_x \chi\big) + \kappa G\big(AI_\tau^{1-\alpha}\Psi_n, \chi\big) \\ &\qquad\qquad = \kappa G\big(AI_\tau^{1-\alpha}\partial_x U_n, \chi\big) + \big(g_n, \chi\big). \end{aligned} \tag{41}$$

We introduce the following useful lemmas for the error analysis of the proposed numerical scheme.

Lemma 4 *[26] The discrete fractional integral $I_\tau^{1-\alpha}\psi_n$ defined in (36) could be rewritten for $1 \le n \le N$*

$$I_\tau^{1-\alpha}\psi_n = c_{n,0}\psi_0 + \sum_{j=1}^{n} b_{n,j}\psi_j, \quad b_{n,j} = \frac{1}{\tau}\int_{t_{n-1}}^{t_n}\int_{t_{j-1}}^{\min(t_j,t)} \beta(t-s)dsdt. \tag{42}$$

Remark 1 As we will see in the derivations in (43), Lemma 4 will be applied to convert the discrete convolution sum into its continuous analogue such that the properties of the fractional integral could be used to obtain the coercivity, which in turn supports the error estimates.

Lemma 5 *For $v, \chi, \hat{\chi} \in \hat{L}^2(0,T;L^2)$ with $v_0 = \chi_0 = \hat{\chi}_0 = 0$, $0 < B_* \le B(x) < \infty$ and $0 < |D(x)| \le D_* < \infty$ for $x \in [0,l]$, the following estimates hold*

$$\begin{aligned} &\tau\sum_{n=1}^{n_*}\big(BI_\tau^{1-\alpha}v_n, v_n\big) \ge B_*\cos\left(\frac{(1-\alpha)\pi}{2}\right)S_{v,n_*}, \ S_{v,n_*} := \big\|{}_0I_t^{\frac{1-\alpha}{2}}\overline{v}\big\|^2_{L^2(0,t_{n_*};L^2)}, \\ &\left|\tau\sum_{n=1}^{n_*}\big(DI_\tau^{1-\alpha}\hat{\chi}_n, \chi_n\big)\right| \le \varepsilon\cos\left(\frac{(1-\alpha)\pi}{2}\right)S_{\chi,n_*} + Q_1\|\hat{\chi}\|^2_{\hat{L}^2(0,t_{n_*};L^2)} \end{aligned}$$

for $1 \le n_* \le N$, for some $\varepsilon > 0$ and for some $Q_1 = Q_1(\varepsilon, D_*)$. Here $\overline{v}$ is defined piecewisely by $\overline{v} = v_j$ for $t \in (t_{j-1}, t_j]$ for $1 \le j \le N$.

Proof We apply (42) and Lemmas 1 and 2 to get

$$\begin{aligned} &\tau\sum_{n=1}^{n_*}\big(BI_\tau^{1-\alpha}v_n, v_n\big) = \tau\sum_{n=1}^{n_*}\sum_{j=1}^{n} b_{n,j}\big(Bv_j, v_n\big) \\ &= \sum_{n=1}^{n_*}\sum_{j=1}^{n}\int_{t_{n-1}}^{t_n}\int_{t_{j-1}}^{\min(t,t_j)}\beta(t-s)\big(B\overline{v}(\cdot,s), v_n\big)dsdt \\ &= \sum_{n=1}^{n_*}\int_{t_{n-1}}^{t_n}\int_0^t \beta(t-s)\big(B\overline{v}(\cdot,s), v_n\big)dsdt \\ &= \int_0^{t_{n_*}}\big(B\,{}_0I_t^{1-\alpha}\overline{v}, \overline{v}\big)dt = \int_0^{t_{n_*}}\big(B\,{}_0I_t^{\frac{1-\alpha}{2}}\overline{v}, {}_tI_{t_{n_*}}^{\frac{1-\alpha}{2}}\overline{v}\big)dt \\ &\ge B_*\cos\left(\frac{(1-\alpha)\pi}{2}\right)\big\|{}_0I_t^{\frac{1-\alpha}{2}}\overline{v}\big\|^2_{L^2(0,t_{n_*};L^2)} = B_*\cos\left(\frac{(1-\alpha)\pi}{2}\right)S_{v,n_*}, \end{aligned} \tag{43}$$

which proves the first inequality of this lemma. We then follow a similar procedure in (43) and apply Lemma 1 to obtain

$$\begin{aligned}
\Big|\tau\sum_{n=1}^{n_*}\big(D I_\tau^{1-\alpha}\hat{\chi}_n,\chi_n\big)\Big| &= \Big|\int_0^{t_{n_*}}\big(D\,{}_0I_t^{1-\alpha}\overline{\hat{\chi}},\overline{\chi}\big)dt\Big| \\
&= \Big|\int_0^{t_{n_*}}\big(D\,{}_0I_t^{\frac{1-\alpha}{2}}\overline{\hat{\chi}},{}_tI_{t_{n_*}}^{\frac{1-\alpha}{2}}\overline{\chi}\big)dt\Big| \\
&\le \varepsilon\cos\left(\frac{(1-\alpha)\pi}{2}\right)\int_0^{t_{n_*}}\big\|{}_0I_t^{\frac{1-\alpha}{2}}\overline{\chi}\big\|^2dt+\frac{Q}{\varepsilon}\int_0^{t_{n_*}}\big\|{}_0I_t^{\frac{1-\alpha}{2}}\overline{\hat{\chi}}\big\|^2dt \\
&\le \varepsilon\cos\left(\frac{(1-\alpha)\pi}{2}\right)S_{\chi,n_*}+\frac{Q}{\varepsilon}\int_0^{t_{n_*}}\big\|\overline{\hat{\chi}}\big\|^2dt \\
&= \varepsilon\cos\left(\frac{(1-\alpha)\pi}{2}\right)S_{\chi,n_*}+\frac{Q}{\varepsilon}\|\hat{\chi}\|^2_{\hat{L}^2(0,t_{n_*};L^2)},
\end{aligned}$$

which proves the second inequality of this lemma. □

5 Error Estimate

Let $\eta = u - \Pi_A u$, $\xi_n = \Pi_A u(x,t_n) - U_n$, $\hat{\eta} = \psi - \Pi_I\psi$ and $\hat{\xi}_n = \Pi_I\psi(x,t_n) - \Psi_n$. We first estimate the truncation errors in the following theorem.

Theorem 3 *If $\breve{w}_0, \breve{\theta}_0 \in H^2$, $q \in H^2(0,T;L^2)$ with $\partial_x q(x,0) \in L^2(0,l)$, $A, I \in W^{1,\infty}(0,l)$ with $A_* \le A(x), I(x) \le A^*$, then the following estimates hold*

$$\begin{aligned}
&\big\|E_u\big\|_{\hat{L}^\infty(L^2)} + \big\|E_\psi\big\|_{\hat{L}^\infty(L^2)} + \|\eta\|_{\hat{L}^\infty(L^2)} + \|\hat{\eta}\|_{\hat{L}^\infty(L^2)} \\
&\qquad + \big\|\delta_\tau\eta\big\|_{\hat{L}^\infty(L^2)} + \big\|\delta_\tau\hat{\eta}\big\|_{\hat{L}^\infty(L^2)} \le QM(\tau+h^2), \\
&\big\|R_{\partial_x(I\partial_x\psi)}\big\|_{\hat{L}^\infty(L^2)} + \big\|R_{\partial_x(A\partial_x u - A\psi)}\big\|_{\hat{L}^\infty(L^2)} + \big\|R_{A(\partial_x u-\psi)}\big\|_{\hat{L}^\infty(L^2)} \le QM\tau,
\end{aligned}$$

where the constant $M := \|\breve{w}_0\|_{H^2} + \|\breve{\theta}_0\|_{H^2} + \|q\|_{H^2(0,T;L^2)} + \|\partial_x q(x,0)\|$.

Proof We apply Theorem 1 to bound E_u in (35) by

$$\|E_u\|_{\hat{L}^\infty(L^2)} \le \max_{1\le n\le N} Q\int_{t_{n-1}}^{t_n}\big\|\partial_t^2 u(\cdot,t)\big\|dt \le Q\tau\|u\|_{W^{2,\infty}(0,T;L^2)} \le QM\tau, \tag{44}$$

and E_ψ can be bounded similarly. We apply (38) with Theorem 2 and $0 \le |G_j(\theta;s)| \le 1$ for $t_{j-1} \le \theta, s \le t_j$, to bound $R_{\partial_x(I\partial_x\psi)}$ by

$$\begin{aligned}
&\|R_{\partial_x(I\partial_x\psi)}\|_{\hat{L}^\infty(L^2)} \\
&\le Q\max_{1\le n\le N}\sum_{j=1}^{n}\int_{t_{j-1}}^{t_j}\frac{\int_{t_{j-1}}^{t_j}\big|G_j(\theta;s)\big|\big\|\partial_\theta\psi(\cdot,\theta)\big\|_{H^2}d\theta}{\Gamma(1-\alpha)(t_n-s)^\alpha}ds \\
&\le QM\max_{1\le n\le N}\sum_{j=1}^{n}\int_{t_{j-1}}^{t_j}\int_{t_{j-1}}^{t_j}\frac{1}{(t_n-s)^\alpha}d\theta ds \\
&\le QM\tau\max_{1\le n\le N}\sum_{j=1}^{n}((t_n-t_{j-1})^{1-\alpha}-(t_n-t_j)^{1-\alpha}) \le QMT^{1-\alpha}\tau \le QM\tau.
\end{aligned} \tag{45}$$

Similarly, the terms $R_{\partial_x(A\partial_x u-A\psi)}$, $R_{A(\partial_x u-\psi)}$ and $R_{\partial_x(I\partial_x\psi)}$ could be bounded as (45). We then use Theorem 2, (40) and the estimate $\|u\|_{C([0,T];H^2)} \le Q\|u\|_{W^{1,\infty}(0,T;H^2)}$ to bound

$$\begin{aligned}
&\|\eta\|_{\hat{L}^\infty(L^2)} \le Qh^2\|u\|_{C([0,T];H^2)} \le QMh^2,\\
&\|\delta_\tau\eta\|_{\hat{L}^\infty(L^2)} \le \tau^{-1}\max_{1\le n\le N}\int_{t_{n-1}}^{t_n}\|\partial_t\eta(\cdot,t)\|dt\\
&\qquad\le Qh^2\tau^{-1}\max_{1\le n\le N}\int_{t_{n-1}}^{t_n}\|\partial_t u(\cdot,t)\|_{H^2}dt \le QMh^2.
\end{aligned}$$

The terms $\|\hat{\eta}\|_{\hat{L}^\infty(L^2)}$ and $\|\delta_\tau\hat{\eta}\|_{\hat{L}^\infty(L^2)}$ could be bounded similarly and thus we complete the proof. □

We then prove the error estimates of the finite element scheme (41).

Theorem 4 *Suppose $\breve{w}_0, \breve{\theta}_0 \in H^2$, $q \in H^2(0,T;L^2)$ with $\partial_x q(x,0) \in L^2(0,l)$. Then the error estimate holds for the fully-discrete finite element scheme* (41)

$$\|U-u\|_{\hat{L}^\infty(0,T;L^2)} + \|\Psi-\psi\|_{\hat{L}^\infty(0,T;L^2)} \le QM(\tau+h^2), \tag{46}$$

where $Q = Q(\rho, A_*, A^*, \|A\|_{W^{1,\infty}}, \|I\|_{W^{1,\infty}}, \kappa, G, E, \alpha, T)$ and M is given in Theorem 3.

Proof We decompose $u_n - U_n = \xi_n + \eta_n$ with $\xi_n = \Pi_A u_n - U_n \in S_h$ and $\psi_n - \Psi_n = \hat{\xi}_n + \hat{\eta}_n$ with $\hat{\xi}_n = \Pi_I\psi_n - \Psi_n \in S_h$. We subtract (41) from the weak formulation and choose $\chi = \xi_n$ and $\hat{\xi}_n$ in the first and the second resulting equations, respectively, to obtain the error equations

$$\begin{aligned}
&\rho\big(A\delta_\tau\xi_n,\xi_n\big) + \kappa G\big(AI_\tau^{1-\alpha}\partial_x\xi_n,\partial_x\xi_n\big)\\
&\quad= \kappa G\big(AI_\tau^{1-\alpha}\hat{\xi}_n,\partial_x\xi_n\big) + \kappa G\big(AI_\tau^{1-\alpha}\hat{\eta}_n,\partial_x\xi_n\big)\\
&\qquad+\big(\kappa G R_{\partial_x(A\partial_x u-A\psi),n} - \rho A\delta_\tau\eta_n - \rho AE_{u,n},\xi_n\big),\\
&\rho\big(I\delta_\tau\hat{\xi}_n,\hat{\xi}_n\big) + E\big(I\,I_\tau^{1-\alpha}\partial_x\hat{\xi}_n,\partial_x\hat{\xi}_n\big) + \kappa G\big(AI_\tau^{1-\alpha}\hat{\xi}_n,\hat{\xi}_n\big)\\
&\quad= \kappa G\big(AI_\tau^{1-\alpha}\partial_x\xi_n,\hat{\xi}_n\big) + \kappa G\big(AI_\tau^{1-\alpha}\big(\partial_x\eta_n-\hat{\eta}_n\big),\hat{\xi}_n\big)\\
&\qquad+\big(ER_{\partial_x(I\partial_x\psi),n} + \kappa G R_{A(\partial_x u-\psi),n} - \rho I\delta_\tau\hat{\eta}_n - \rho IE_{\psi,n},\hat{\xi}_n\big).
\end{aligned} \tag{47}$$

We multiply (47) by 2τ, use the relation $\big(AI_\tau^{1-\alpha}\partial_x v_n,\hat{\xi}_n\big) = -\big(I_\tau^{1-\alpha}Av_n,\partial_x\hat{\xi}_n\big) - \big((\partial_x A)I_\tau^{1-\alpha}v_n,\hat{\xi}_n\big)$ for $v = \xi$ and η, and then apply the geometric-arithmetic inequality to obtain

$$\begin{aligned}
&\rho\big\|\sqrt{A}\xi_n\big\|^2 + 2\tau\kappa G\big(AI_\tau^{1-\alpha}\partial_x\xi_n,\partial_x\xi_n\big)\\
&\quad\le \rho\big\|\sqrt{A}\xi_{n-1}\big\|^2 + 2\tau\kappa G\big(AI_\tau^{1-\alpha}(\hat{\xi}_n+\hat{\eta}_n),\partial_x\xi_n\big) + \tau\big\|G_{1,n}\big\|^2 + \tau\big\|\xi_n\big\|^2,\\
&\rho\big\|\sqrt{I}\hat{\xi}_n\big\|^2 + 2\tau E\big(I\,I_\tau^{1-\alpha}\partial_x\hat{\xi}_n,\partial_x\hat{\xi}_n\big) + 2\tau\kappa G\big(AI_\tau^{1-\alpha}\hat{\xi}_n,\hat{\xi}_n\big)\\
&\quad\le \rho\big\|\sqrt{I}\hat{\xi}_{n-1}\big\|^2 - 2\tau\kappa G\big(AI_\tau^{1-\alpha}\xi_n,\partial_x\hat{\xi}_n\big) - 2\tau\kappa G\big((\partial_x A)I_\tau^{1-\alpha}\xi_n,\hat{\xi}_n\big)\\
&\qquad-2\tau\kappa G\big(AI_\tau^{1-\alpha}\eta_n,\partial_x\hat{\xi}_n\big) - 2\tau\kappa G\big(I_\tau^{1-\alpha}\big(A\hat{\eta}_n+(\partial_x A)\eta_n\big),\hat{\xi}_n\big)\\
&\qquad+\tau\big\|G_{2,n}\big\|^2 + \tau\big\|\hat{\xi}_n\big\|^2,
\end{aligned} \tag{48}$$

where $G_{1,n} = \kappa G R_{\partial_x(A\partial_x u-A\psi),n} - \rho A\delta_\tau\eta_n - \rho AE_{u,n}$, and $G_{2,n} = ER_{\partial_x(I\partial_x\psi),n} + \kappa G R_{A(\partial_x u-\psi),n} - \rho I\delta_\tau\hat{\eta}_n - \rho IE_{\psi,n}$ for $1 \le n \le N$. We add the first inequality in (48) from

$n = 1$ to n_0 for $1 \le n_0 \le N$ and apply Theorem 3 and Lemma 5 to get

$$\begin{aligned}
&\rho A_* \|\xi_{n_0}\|^2 + 2\kappa G A_* \cos\left(\frac{(1-\alpha)\pi}{2}\right) S_{\partial_x \xi, n_0} \\
&\le \kappa G A_* \cos\left(\frac{(1-\alpha)\pi}{2}\right) S_{\partial_x \xi, n_0} + Q\tau \sum_{n=1}^{n_0} \left(\|\xi_n\|^2 + \|\hat{\xi}_n\|^2 + \|\hat{\eta}_n\|^2\right) \\
&\quad + QM^2(\tau^2 + h^4).
\end{aligned} \tag{49}$$

We apply Lemma 5 to estimate the terms on the right-hand side of the second inequality in (48) as follows

$$\begin{aligned}
&\Big| \sum_{n=1}^{n_0} \big[-2\tau\kappa G\big(A I_\tau^{1-\alpha} \xi_n, \partial_x \hat{\xi}_n\big) - 2\tau\kappa G\big((\partial_x A) I_\tau^{1-\alpha} \xi_n, \hat{\xi}_n\big) \\
&\quad -2\tau\kappa G\big(A I_\tau^{1-\alpha} \eta_n, \partial_x \hat{\xi}_n\big) - 2\tau\kappa G\big(I_\tau^{1-\alpha}\big(A\hat{\eta}_n + (\partial_x A)\eta_n\big), \hat{\xi}_n\big)\big] \Big| \\
&\quad \le E A_* \cos\left(\frac{(1-\alpha)\pi}{2}\right) S_{\partial_x \hat{\xi}, n_0} + \kappa G A_* \cos\left(\frac{(1-\alpha)\pi}{2}\right) S_{\hat{\xi}, n_0} \\
&\qquad + Q\tau \sum_{n=1}^{n_0} (\|\xi_n\|^2 + \|\eta_n\|^2 + \|\hat{\eta}_n\|^2),
\end{aligned}$$

and we incorporate this with a similar derivation as (49) for the second inequality of (48) to get

$$\begin{aligned}
&\rho A_* \|\hat{\xi}_{n_0}\|^2 + 2E A_* \cos\left(\frac{(1-\alpha)\pi}{2}\right) S_{\partial_x \hat{\xi}, n_0} + 2\kappa G A_* \cos\left(\frac{(1-\alpha)\pi}{2}\right) S_{\hat{\xi}, n_0} \\
&\le E A_* \cos\left(\frac{(1-\alpha)\pi}{2}\right) S_{\partial_x \hat{\xi}, n_0} + \kappa G A_* \cos\left(\frac{(1-\alpha)\pi}{2}\right) S_{\hat{\xi}, n_0} \\
&\quad + Q\tau \sum_{n=1}^{n_0} \left(\|\xi_n\|^2 + \|\hat{\xi}_n\|^2 + \|\eta_n\|^2 + \|\hat{\eta}_n\|^2\right) + QM^2(\tau^2 + h^4).
\end{aligned} \tag{50}$$

We add (49) and (50) and use Theorem 3 to obtain for $1 \le n_0 \le N$

$$\begin{aligned}
&\rho \|\xi_{n_0}\|^2 + \rho \|\hat{\xi}_{n_0}\|^2 + \cos\left(\frac{(1-\alpha)\pi}{2}\right)\left(\kappa G S_{\partial_x \xi, n_0} + E S_{\partial_x \hat{\xi}, n_0} + \kappa G S_{\hat{\xi}, n_0}\right) \\
&\le QM^2(\tau^2 + h^4) + Q\tau \sum_{n=1}^{n_0} \left(\|\xi_n\|^2 + \|\hat{\xi}_n\|^2\right).
\end{aligned} \tag{51}$$

We choose τ sufficiently small and apply the discrete Gronwall's inequality for (51) to obtain for $1 \le n \le N$

$$\|\xi_n\| + \|\hat{\xi}_n\| \le QM(\tau + h^2). \tag{52}$$

We combine (52) with (40) to complete the proof. □

Remark 2 In the current study we only consider the first-order temporal discretization scheme due to the complexity of higher-order regularity estimates of the solutions to the coupled system, while the Crank-Nilcolson time discretization scheme in combination with the averaged product-integration rule for the fractional integral [4, 26, 30] could be applied to construct the second-order temporal approximation. In particular, nonuniform temporal meshes could be used to account for the solution singularity to recover the second-order accuracy.

6 Numerical Experiments

We carry out numerical experiments to investigate the convergence behavior of the scheme (41) to model (16) and the performance of the proposed viscoelastic Timoshenko beam model in the context of real isotropic material, in comparison with its integer-order analogue

$$\begin{aligned} \rho A(x)\partial_t^2 w &= \partial_x\big(\kappa G A(x)\big(\partial_x w-\theta\big)\big)+q(x,t),\\ \rho I(x)\partial_t^2\theta &= \partial_x\big(EI(x)\partial_x\theta\big)+\kappa G A(x)\big(\partial_x w-\theta\big) \end{aligned} \tag{53}$$

with initial and boundary conditions in (3)–(4), the integer-order Euler-Bernoulli beam

$$\begin{aligned} &\rho A(x)\partial_t^2 w+\partial_x^2\big(EI(x)\partial_x^2 w\big)=q(x,t), \quad (x,t)\in(0,l)\times(0,T],\\ &w(0,t)=\partial_x w(0,t)=w(l,t)=\partial_x w(l,t)=0, \quad t\in[0,T],\\ &w(x,0)=\partial_t w(x,0)=0, \quad x\in[0,l], \end{aligned} \tag{54}$$

and the fractional Euler-Bernoulli beam model

$$\rho A(x)\partial_t^2 w+\partial_x^2\big(EI(x)\partial_t^\alpha\partial_x^2 w\big)=q(x,t) \tag{55}$$

with initial and boundary conditions in (54). Both the spatial and temporal partitions are uniform with the mesh sizes h and τ, respectively.

6.1 Convergence Rate of the Finite Element Scheme

Let $[0,l]\times[0,T]=[0,1]\times[0,1]$ and $\rho=A(x)=E=I(x)=\kappa=G=1$ for simplicity. We assume homogeneous initial conditions and the uniform pressure load $q=0.01$ within the beam. Since the explicit solution of the fractional Timoshenko beam model (1) are in general not available, we use the numerical solution $\hat{U}$ and $\hat{\Psi}$ computed under $(\tau,h)=(1/1440,1/720)$ as the reference solution to test the temporal convergence rates, and the numerical solution computed under $(\tau,h)=(1/1024,1/720)$ as the reference solution to test the spatial convergence rates. Therefore, we compute the convergence orders r, $\hat{r}$, ι and $\hat{\iota}$ of the following errors

$$\|U-\hat{U}\|_{\hat{L}^\infty(0,T;L^2)}\le Q\big(\tau^r+h^\iota\big), \quad \|\Psi-\hat{\Psi}\|_{\hat{L}^\infty(0,T;L^2)}\le Q\big(\tau^{\hat{r}}+h^{\hat{\iota}}\big), \tag{56}$$

and numerical results are presented in Tables 1, 2, 3, which indicates the first-order accuracy in time and the second-order accuracy in space of the scheme (41) and thus substantiates the theoretical analysis.

6.2 Dynamic Response of Timoshenko Beam Models

The dynamic durability provides experimental evidence that the beam structures can survive a specific dynamic environment. In this case, a test structure is driven or forced to vibrate by specified inputs, e.g, natural frequencies. Therefore, it is of great importance to precisely predict and describe the resonance behaviors of the mechanical structures. In this subsection, the high-strength, corrosion-resistant nickel chromium alloy 718 material [49] is selected for dynamic investigation of the beams. This age-hardenable alloy is readily fabricated to provide outstanding fatigue resistance, a wide range of temperature creep strength and rupture strength. This superalloy beam has a weight density of $\rho=8192$ kg/m^3, a modulus of elasticity of $E=200$ GPa, a shear modulus of $G=80$ GPa, and a Timoshenko shear coefficient $\kappa=5/6$ [49]. The beams are set to have length $l=1$m and width 0.1m. The

Table 1 Temporal convergence rates for scheme (41)

$\|U-\hat{U}\|_{\hat{L}^\infty(L^2)}$	τ	$\alpha=0.3$		$\alpha=0.5$		$\alpha=0.7$	
	1/32	1.49E-08	–	8.19E-06	–	2.05E-06	–
	1/48	9.84E-09	1.03	5.54E-06	0.96	1.35E-06	1.02
	1/64	7.29E-09	1.04	4.16E-06	1.00	1.00E-06	1.05
	1/72	6.45E-09	1.05	3.68E-06	1.02	8.84E-07	1.06
	1/96	4.75E-09	1.06	2.72E-06	1.05	6.48E-07	1.08
$\|\Psi-\hat{\Psi}\|_{\hat{L}^\infty(L^2)}$	1/32	1.25E-11	–	6.93E-07	–	1.77E-07	–
	1/48	8.22E-12	1.04	4.68E-07	0.97	1.17E-07	1.03
	1/64	6.08E-12	1.05	3.51E-07	1.00	8.66E-08	1.05
	1/72	5.37E-12	1.06	3.11E-07	1.03	7.64E-08	1.06
	1/96	3.95E-12	1.07	2.30E-07	1.05	5.60E-08	1.08

Table 2 Spatial convergence rates for scheme (41)

$\|U-\hat{U}\|_{\hat{L}^\infty(L^2)}$	h	$\alpha=0.3$		$\alpha=0.5$		$\alpha=0.7$	
	1/8	4.67E-06	–	2.52E-06	–	5.98E-07	–
	1/16	1.14E-06	2.04	6.22E-07	2.02	1.47E-07	2.02
	1/24	5.02E-07	2.01	2.76E-07	2.01	6.53E-08	2.01
	1/36	2.23E-07	2.01	1.22E-07	2.01	2.89E-08	2.01
	1/40	1.80E-07	2.01	9.89E-08	2.01	2.34E-08	2.01
$\|\Psi-\hat{\Psi}\|_{\hat{L}^\infty(L^2)}$	1/8	1.21E-06	–	3.04E-07	–	2.67E-08	–
	1/16	3.16E-07	1.94	7.64E-08	2.00	6.89E-09	1.95
	1/24	1.41E-07	1.98	3.39E-08	2.00	3.08E-09	1.99
	1/36	6.29E-08	1.99	1.51E-08	2.00	1.37E-09	2.00
	1/40	5.10E-08	2.00	1.22E-08	2.01	1.11E-09	2.00

thicknesses of the slender and thick beams are $h_s = 0.025$m and $h_t = 0.2$m, where s and t denote the slender and thick beams, respectively, which give the primary natural frequencies for Timoshenko beams as $\omega_1^{timo,s} = 794$ rad/s and $\omega_1^{timo,t} = 5006$ rad/s [35]. In the numerical experiments, we choose the loading term $q = B\cos(\omega t)\delta(x - \frac{l}{2})$ located at the middle of the beam, with $B_s^{timo} = B_t^{timo} = 1$ and the excitation frequency $\omega = \omega_1^{timo,s}, \omega_1^{timo,t}$ over a time interval $[0, T] = [0, 1\text{s}]$.

The Timoshenko beam models are simulated via the finite element scheme (41) with $h = 1/4096$. Due to the high temporal frequency of the given load term, the numerical approximation with deficient temporal partitions cannot catch the resonance phenomenon described by the physical model, and often results in spurious and nonphysical phenomena "beat", i.e., the vibration is a rapid oscillation with slowly varying amplitude [14], which is in sharp contrast with the diffusion models. In Fig. 2, we investigate the resonance behaviors of the center of neutral beam axis over a short time period $[0, T] = [0, 0.1\text{s}]$, which indicates that fine temporal mesh is required to produce the physical behaviors for the fixed observation time.

Table 3 The rotational angles for Euler-Bernoulli beams and Timoshenko beams

		Slender beam			Thick beam		
$\alpha = 0$	x	ζ_{euler}	ζ_{timo}	$\zeta_{timo,b}$	ζ_{euler}	ζ_{timo}	$\zeta_{timo,b}$
$B_t^{euler} = 1$	$l/8$	-2.70E-06	-2.69E-06	-2.67E-06	2.97E-06	-3.10E-06	-1.95E-06
$B_t^{timo} = 1$	$l/4$	-3.22E-06	-3.26E-06	-3.24E-06	3.61E-06	-3.30E-06	-2.37E-06
	$3l/4$	3.22E-06	3.26E-06	3.24E-06	-3.61E-06	3.30E-06	2.37E-06
	$7l/8$	2.70E-06	2.69E-06	2.67E-06	-2.97E-06	3.10E-06	1.95E-06
$\alpha = 0.1$	x	ζ_{euler}	ζ_{timo}	$\zeta_{timo,b}$	ζ_{euler}	ζ_{timo}	$\zeta_{timo,b}$
$B_t^{euler} = 1000$	$l/8$	-1.47E-07	1.55E-07	1.53E-07	-1.46E-07	1.68E-07	1.07E-07
$B_t^{timo} = 600$	$l/4$	-1.83E-07	1.92E-07	1.91E-07	-1.84E-07	1.86E-07	1.35E-07
	$3l/4$	1.83E-07	-1.92E-07	-1.91E-07	1.84E-07	-1.86E-07	-1.35E-07
	$7l/8$	1.47E-07	-1.55E-07	-1.53E-07	1.46E-07	-1.68E-07	-1.07E-07
$\alpha = 0.9$	x	ζ_{euler}	ζ_{timo}	$\zeta_{timo,b}$	ζ_{euler}	ζ_{timo}	$\zeta_{timo,b}$
$B_t^{euler} = 4000$	$l/8$	-1.09E-09	-1.10E-09	-1.09E-09	-1.31E-09	-1.22E-09	-8.13E-10
$B_t^{timo} = 2000$	$l/4$	-1.45E-09	-1.47E-09	-1.46E-09	-1.74E-09	-1.50E-09	-1.08E-09
	$3l/4$	1.45E-09	1.47E-09	1.46E-09	1.74E-09	1.50E-09	1.08E-09
	$7l/8$	1.09E-09	1.10E-09	1.09E-09	1.31E-09	1.22E-09	8.13E-10

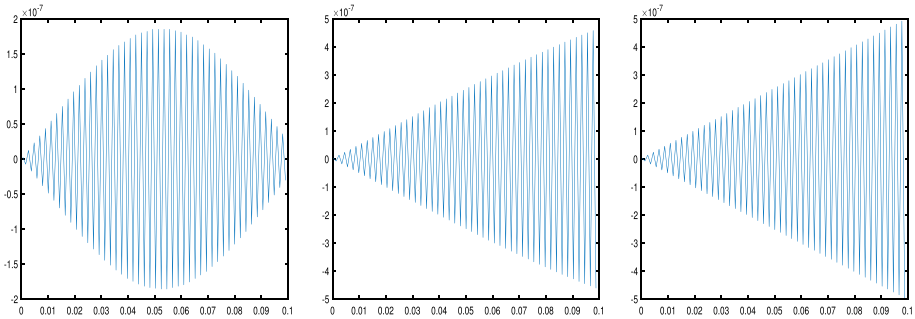

Fig. 2 Left to right: Displacement of the thick integer-order Timoshenko beam (53) on $[0, T]$ for $T = 0.1$s with $\tau = \frac{\pi}{8\omega}$, $\tau = \frac{\pi}{16\omega}$, and $\tau = \frac{\pi}{32\omega}$, respectively

In Fig. 3, we display the time history of the transverse displacement of the neutral beam axis with the same data as in Fig. 2. To properly present the temporal evolution with the fine time resolution, we alternatively sample the maximum and minimum every $1\frac{1}{2}$ time periods. The very fine temporal step $\tau = \frac{\pi}{1024\omega}$ is applied to ensure the time resolution to generate physically relevant observations. When the external driving frequency equals to the natural frequency of the beams, we observe from Fig. 3 that (1) the predicted vibrations of the integer-order Timoshenko beam grow linearly in time, which is not consistent with the physical observations since they do not take damping effects into consideration. In contrast, (2) the maximum amplitude of the slender Timoshenko beams ranges from 8×10^{-5} for integer-order model (53) to 1×10^{-7} for fractional model (1) with $\alpha = 0.1$, and decreases further from 1×10^{-7} to 5×10^{-10} with α increasing from 0.1 to 0.9, which are consistent with the discussions in §1. Furthermore, (3) the fractional operator in the fractional Timoshenko beam model naturally incorporates the viscoelastic damping mechanism and thus predicts

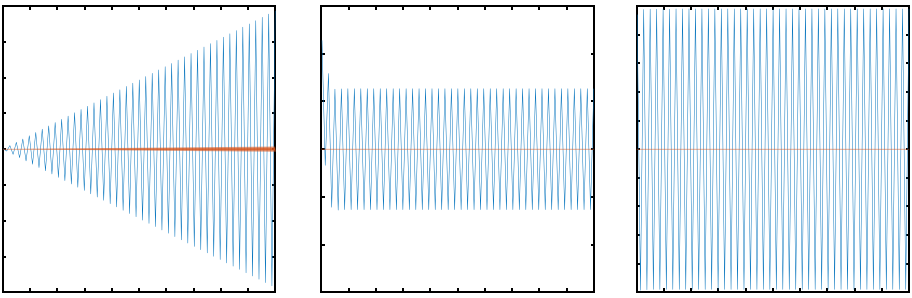

Fig. 3 Left to right: Deflection of the integer-order Timoshenko beams and fractional Timoshenko beams for $\alpha = 0.1$, and $\alpha = 0.9$, on $[0, T]$ for $T = 1$s. Blue line: Slender beam. Red line: Thick beam (Color figure online)

vibrations that do not oscillate infinitely, which agrees more with physical observations [17, 40].

6.3 Model Comparison in Terms of the Total Angle of Rotation

We compare the total angles of rotation of integer-order and fractional Euler-Bernoulli and Timoshenko beams as shown in Fig. 1. We choose the same material as §6.2 and apply the same parameters of the Timoshenko beam therein. Euler-Bernoulli beams are set to have length l =1 m and width 0.1m with $h_s = 0.025$m and $h_t = 0.2$m, and the primary natural frequencies for Euler-Bernoulli beams are $\omega_1^{euler,s} = 798$ rad/s and $\omega_1^{euler,t} = 6381$ rad/s [35]. The loading term in §6.2 are specified with $\omega = \omega_1^{euler,s}$ and $\omega_1^{euler,t}$ over a time interval $[0, T] = [0, 1\text{s}]$. The Euler-Bernoulli models are simulated via cubic Hermite finite element method with 64 elements. The rotational angles illustrated in Fig. 1 for the Euler-Bernoulli beams are computed by $\zeta_{euler} = \zeta_{euler,b} = \partial_x w$, and those for the Timoshenko beams are evaluated by $\zeta_{timo} = \partial_x w$ and $\zeta_{timo,s} = \zeta_{timo} - \zeta_{timo,b} = \partial_x w - \theta$.

To better present the effects of the shear deformation, we apply the amplitude of the loading term $B_s = 1$ for slender beams and adjust B_t for thick beams accordingly to compare these angles at the time when slender beams and thick beams exhibit similar total rotation angle ζ of the same magnitude. We present the angles ζ_{euler} of Euler-Bernoulli beams and ζ_{timo} and $\zeta_{timo,b}$ of the Timoshenko beams measured at different spatial locations in Table 3 with the same τ, h, $\omega_1^{timo,s}$ and $\omega_1^{timo,t}$ as those in Fig. 3.

Table 3 shows that for the case of slender beams with almost the same total rotation angles $\zeta_{euler} \approx \zeta_{timo}$, both integer-order (i.e. $\alpha = 0$) and fractional-order (i.e. $\alpha > 0$) Timoshenko beams generate $\zeta_{timo,s}/\zeta_{timo} \approx 0.7\%$, which indicates that the contribution of the shear deformation on the rotational angles is negligible such that the rotational angles of both Euler-Bernoulli and Timoshenko beams are almost due to bending. In other words, both of the models generate similar results for the case of slender beams. However, for the case of thick beams with $\zeta_{euler} \approx \zeta_{timo}$, $\zeta_{timo,s}/\zeta_{timo} \approx 35\%$ in the Timoshenko beam models, which implies that the shear deformation has significant impacts for the rotational angles of the thick beams and thus the bending behavior depicted by the Timoshenko model deviates from that by the Euler-Bernoulli model and is indeed more reasonable due to the consideration of shear deformation.

7 Concluding Rmarks

In this work we prove high-order regularity of the solutions to a fractional Timoshenko beam model, and then derive and analyze its fully-discrete finite element scheme without any regularity assumption of its true solutions, but only on the data. Numerical experiments indicate that the fractional Timoshenko model not only retains major advantages of its integer-order analogue such as accounting for the impacts of the shear deformation for the rotational angles, but provides an more adequate modeling for the mechanical vibrations of thick beams, composite beams and beams under high frequency excitations, in comparison with Euler-Bernoulli beam models.

From the perspective of physical properties, the integer-order Timoshenko beam model for purely elastic materials without damping effects follows the energy conservation property but might result in inaccurate approximations for long observation time due to the lack of damping effects [14, 35]. To accommodate this issue, there exist several models accounting for the damping effects for the integer-order Timoshenko beam model, e.g. linear frictional dampings in the form of first-order derivatives [29, 36, 39]. Nevertheless, these systems tend to generate exponential decay of the energy and might not produce precise approximations of the experimentally observed power-law behaviors of the viscoelastic materials over a wide parameter range [2, 15, 24, 34]. In contrast, the fractional Timoshenko beam model could robustly describe the observed power-law behaviors of the viscoelastic materials with numerous experimental demonstrations [8, 33, 40], and provides more modeling flexibility via different choices of the fractional order α for different beams. More rigorous investigations and comparisons for physical properties of integer-order and fractional Timoshenko beam models will be considered in the near future.

Acknowledgements The authors would like to express their most sincere thanks to the referees for their very constructive and helpful comments and suggestions, which greatly improved the quality of this paper. This work was partially supported by the National Science Foundation under Grant No. DMS-2012291 and the National Natural Science Foundation of China under Grant No. 11971272. Enquiries about data availability should be directed to the authors.

Declarations

conflict of interest The authors declare that they have no conflict of interest.

References

1. Adams, R., Fournier, J.: Sobolev Spaces. Elsevier, New York (2003)
2. Bagley, R.: Power law and fractional calculus model of viscoelasticity. AIAA J. **27**, 1412–1417 (1989)
3. Bonfanti, A., Kaplan, J., Charras, G., Kabla, A.: Fractional viscoelastic models for power-law materials. Soft Matter **16**, 6002–6020 (2020)
4. Chen, H., Qiu, W., Zaky, M., Hendy, A.: A two-grid temporal second-order scheme for the two-dimensional nonlinear Volterra integro-differential equation with weakly singular kernel. Calcolo **60**, 13 (2023)
5. Christensen, R.: Theory of Viscoelasticity: An Introduction. Academic Press, New York (1982)
6. Deng, W., Li, C., Lü, J.: Stability analysis of linear fractional differential system with multiple time delays. Nonlinear Dyn. **48**, 409–416 (2007)
7. Diethelm, K.: The Analysis of Fractional Differential Equations, Ser. Lecture Notes in Mathematics, vol. 2004. Springer-Verlag, Berlin (2010)
8. Eldred, L., Baker, W., Palazotto, A.: Kelvin-Voigt versus fractional derivative model as constitutive relations for viscoelastic materials. AIAA J. **33**, 547–550 (1995)
9. Ervin, V., Roop, J.: Variational formulation for the stationary fractional advection dispersion equation. Numer. Methods Partial Differ. Equ. **22**, 558–576 (2006)

10. Evans, L.: Partial Differential Equations, Grad. Stud. Math. 19, American Mathematical Society, Providence, RI (1998)
11. Gunzburger, M., Li, B., Wang, J.: Convergence of finite element solutions of stochastic partial integro-differential equations driven by white noise. Numer. Math. **141**, 1043–1077 (2019)
12. Guo, Y., Yu, G., Xie, X.: Uniform analysis of a stabilized hybrid finite element method for Reissner-Mindlin plates. Sci. China Math. **56**, 1727–1742 (2013)
13. He, Y., Lin, Y., Shen, S., Sun, W., Tait, R.: Finite element approximation for the viscoelastic fluid motion problem. J. Comput. Appl. Math. **155**, 201–222 (2003)
14. Inman, D.: Engineering Vibrations, 4th edn. Pearson, New Jersey (2014)
15. Jaiseenkar, A., McKinley, G.: Power-law rheology in the bulk and at the interface: quasi-properties and fractional constitutive equations. Proc. R. Soc. A **469**, 20120284 (2013)
16. Jin, B., Lazarov, R., Zhi, Z.: Error estimates for a semidiscrete finite element method for fractional order parabolic equations. SIAM J. Numer. Anal. **51**, 445–466 (2013)
17. Johnson, C., , Kienholz, D: Finite element prediction of damping in structures with constrained viscoelastic layers, 22nd Structures, Structural Dynamics and Materials Conference, Atlanta, USA, April 06-08 (1981)
18. Karaa, S., Pani, A.: Optimal error estimates of mixed FEMs for second order hyperbolic integro-differential equations with minimal smoothness on initial data. J. Comput. Appl. Math. **275**, 113–134 (2015)
19. Kopteva, N.: Error analysis of the L1 method on graded and uniform meshes for a fractional-derivative problem in two and three dimensions. Math. Comput. **88**, 2135–2155 (2019)
20. Liang, H., Brunner, H.: Collocation methods for integro-differential algebraic equations with index 1. IMA J. Numer. Anal. **40**, 850–885 (2020)
21. Lin, Y.: Semi-discrete finite element approximations for linear parabolic integro-differential equations with integrable kernels. J. Integral Equ. Appl. **10**, 51–83 (1998)
22. Lubich, C., Sloan, I., Thomée, V.: Nonsmooth data error estimates for approximations of an evolution equation with a positive-type memory term. Math. Comput. **65**, 1–17 (1996)
23. Mao, Z., Shen, J.: Efficient spectral-Galerkin methods for fractional partial differential equations with variable coefficients. J. Comput. Phys. **307**, 243–261 (2016)
24. Mainardi, F.: Fractional Calculus and Waves in Linear Viscoelasticity: An Introduction to Mathematical Models. Imperial College Press, London (2010)
25. Mainardi, F., Spada, G.: Creep, relaxation and viscosity properties for basic fractional models in rheology. Eur. Phys. J. Spec. Top. **193**, 133–160 (2011)
26. McLean, W., Thomée, V.: Numerical solution of an evolution equation with a positive-type memory term. J. Austral. Math. Soc. Ser. B **35**, 23–70 (1993)
27. McLean, W., Thomée, V., Wahlbin, L.: Discretization with variable time steps of an evolution equation with a positive-type memory term. J. Comput. Appl. Math. **69**, 49–69 (1996)
28. Meirovitch, L.: Fundamentals of Vibrations. McGraw-Hill, New York (2001)
29. Muñoz Rivera, J., Racke, R.: Timoshenko systems with indefinite damping. J. Math. Anal. Appl. **341**, 1068–1083 (2008)
30. Mustapha, K., McLean, W.: Discontinuous Galerkin method for an evolution equation with a memory term of positive type. Math. Comput. **78**, 1975–1995 (2009)
31. Nutting, P.: A new general law of deformation. J. Franklin Inst. **191**, 679–685 (1921)
32. Pani, A., Fairweather, G.: H^1 Galerkin mixed finite element methods for parabolic integro-differential equations. IMA J. Numer. Anal. **22**, 231–252 (2002)
33. Perdikaris, P., Karniadakis, G.: Fractional-order viscoelasticity in one-dimensional blood flow models. Ann. Biomed. Eng. **42**, 1012–1023 (2014)
34. Podlubny, I.: Fractional Differential Equations. Academic Press, New York (1999)
35. Rao, S.: Vibration of continuous systems. John Wiley Sons, Hoboken (2019)
36. Raposo, C., Ferreira, J., Santos, M., Castro, N.: Exponential stability for the Timoshenko system with two weak dampings. Appl. Math. Lett. **18**, 535–541 (2005)
37. Samko, S., Kilbas, A., Marichev, O.: Fractional Integrals and Derivatives: Theory and Applications. Gordon and Breach, New York (1993)
38. Sinha, R., Ewing, R., Lazarov, R.: Mixed finite element approximations of parabolic integro-differential equations with nonsmooth initial data. SIAM J. Numer. Anal. **47**, 3269–3292 (2009)
39. Soufyane, A.: Exponential stability of the linearized nonuniform Timoshenko beam. Nonlinear Anal. Real World Appl. **10**, 1016–1020 (2009)
40. Suzuki, J., Kharazmi, E., Varghaei, P., Naghibolhosseini, M., Zayernouri, M.: Anomalous nonlinear dynamics behavior of fractional viscoelastic beams. J. Comput. Nonlinear Dyn. **16**, 111005 (2021)
41. Suzuki, J., Zhou, Y., D'Elia, M., Zayernouri, M.: A thermodynamically consistent fractional visco-elasto-plastic model with memory-dependent damage for anomalous materials. Comput. Methods Appl. Mech. Engrg. **373**, 113494 (2021)

42. Tatar, N.: Well-posedness and stability for a fractional thermo-viscoelastic Timoshenko problem. Comput. Appl. Math. **40**, 1–34 (2021)
43. Thomée, V.: Galerkin Finite Element Methods for Parabolic Problems. Lecture Notes in Mathematics, vol. 1054. Springer-Verlag, New York (1984)
44. Trask, N., You, H., Yu, Y., Parks, M.: An asymptotically compatible meshfree quadrature rule for nonlocal problems with applications to peridynamics. Comput. Methods Appl. Mech. Eng. **343**, 151–165 (2019)
45. Webb, J.: Weakly singular Gronwall inequalities and applications to fractional differential equations. J. Math. Anal. Appl. **471**, 692–711 (2019)
46. Xu, D.: Analytical and numerical solutions of a class of nonlinear integro-differential equations with L1 kernels. Nonlinear Anal. Real World Appl. **51**, 103002 (2020)
47. Zhao, L., Deng, W., Hesthaven, J.: Characterization of image spaces of Riemann-Liouville fractional integral operators on Sobolev spaces $W^{m,p}(\Omega)$. Sci. China Math. **64**, 2611–2636 (2021)
48. Zheng, X., Li, Y., Wang, H.: A viscoelastic Timoshenko beam: model development, analysis and investigation. J. Math. Phys. **63**, 061509 (2022)
49. Inconel alloy 718, Publication Number SMC-045 Copyright Special Metals Corporation, 2007, www.specialmetals.com